Available online at www.sciencedirect.com
SCIENCE DIRECT®
Journal of Solid State Chemistry 176 (2003) 13–17
JOURNAL OF SOLID STATE CHEMISTRY
http://elsevier.com/locate/jssc

Preparation and characterization of the nanoporous ultrathin multilayer films based on molybdenum polyoxometalate $(Mo_{38})_n$

L. Wang,[a] M. Jiang,[a] E.B. Wang,[a,*] L.Y. Duan,[a] N. Hao,[a] Y. Lan,[a] L. Xu,[a,b] and Z. Li[b]

[a] *Department of Chemistry, Institute of Polyoxometalate Chemistry, Northeast Normal University, Changchun 130024, People's Republic of China*
[b] *Changchun Institute of Applied Chemistry, Academia Sinica, Changchun 130024, People's Republic of China*

Received 11 March 2003; received in revised form 28 April 2003; accepted 6 May 2003

Abstract

Ultrathin multilayer films of the wheel-shaped molybdenum polyoxometalate cluster $(Mo_{38})_n$ and poly(allylamine hydrochloride)(PAH) have been prepared by the layer-by-layer (LbL) self-assembly method. The $((Mo_{38})_n/PAH)_m$ multilayer films have been characterized by X-ray photoelectron spectra (XPS) and atomic force microscopy (AFM). UV–VIS measurements reveal regular film growth with each $(Mo_{38})_n$ adsorption. The electrochemistry behavior of the film at room temperature was investigated.

Keywords: Polyoxometalates; Polyelectrolyte; Layer-by-layer; Ultrathin multilayer film; Electrochemical behavior'

1. Introduction

In the past few years, the fabricaion of self-assembled ultrathin films has attracted considerable interest because of their importance in the design of nanocrystallites, colloidal gold, titanium dioxide, and magnetite nanoparticles and other functional components incorporated into a polymer matrixes [1–8].

Polyoxometalates (POMs) are attractive building blocks for functional material with potential application in electrocatalysis and the preparations of molecular electronic, or electrooptions devices [9,10]. One of the most important properties of these metal oxide clusters is the capability for reversible multivalence reduction, forming mixed-valence species. The property makes them very useful in the preparation of modified electrodes and brings about favorable catalytic proper ties with regard to several challenging electrochemical processes such as the reduction of nitrite. So, how to design new kinds of polyoxometalates and successfully immobilize them on electrode surfaces, while maintaining and enhancing their beneficial properties, is fascinating to chemists. With self-assembly processes involving Mo^V lead to a structurally diverse family of well-defined wheel-shaped nanoparticles or clusters, and it has been shown recently that such compounds can be connected in several different ways to design extended solids [11–13]. Practical applications of polyoxometalates in these areas depend on the successful preparation of thin polyoxometalate-containing films [14,15]. The study was focused mainly on the electrochemical properties of the films. Kurth and Coworkers recently reported the preparation of three ultrathin multilayer POM-polyelectrolyte films, incorporating the POM cluster $(NH_4)_{21}[H_3Mo_{57}V_6(NO)_6O_{183}(H_2O)_{18}]$ and the keplerate cluster $(NH_4)_{42}[Mo_{132}O_{372}(CH_3COO)_{30}(H_2O)_{72}]$ [16–18], as well as polyoxometalate nanoclusters by the LbL method [21]. Their results display that the LBL method is also applicable for fabricating multilayer films of anionic POMs and polycationic PAH, however, the exploration of POM-based multilayer films as functional materials has been rarely demonstrated. For this, it will be of critical importance to successfully incorporate the functional properties of POMs into the ultrathin material. Here we describe LbL multilayer films based on POMs prepared from $(Mo_{38})_n$ and positively charged polyelectrolytes and study electrochemical behavior of $((Mo_{38})_n/PAH)_m$ composite films modified WIGE electrode. Its catalytic and electrocatalytic activity can be retained and even enhanced when it is immobilized on.

*Corresponding author. Fax: +86-431-568-4009.
E-mail address: wangenbo@public.cc.jl.cn (E.B. Wang).

0022-4596/03/$ - see front matter © 2003 Elsevier Inc. All rights reserved.
doi:10.1016/S0022-4596(03)00277-9

2. Experimental

2.1. Materials

The wheel-shaped polyoxomolybdate $\{[H_2O]^{+}_{12}\{(H_2O)MoO_{2.5}[Mo_{36}O_{108}(NO)_4(H_2O)_{16}]O_{2.5}Mo(H_2O)\}^{12-}\}_n$ ($(Mo_{38})_n$), was prepared according to Ref. [19] and was crystallized two times. IR (KBr pellet, ν/cm): 1621 v s, 1405 v s, 950 s, 906 s, 876 v s, 778 m, 626 s, 574 s, 378 m, 221 s cm^{-1} Poly(ethyleneimine) (PEI; MW50,000), poly(styrenesulfonate) (PSS; MW 70,000), and poly(allylamine hydrochloride) (PAH; MW 70000) were purchased from Aldrich and were used without further treatment. Structures of $(Mo_{38})_n$ anion used in this study are shown in Fig. 1. The water used in all experiments was deionized to a resistivity of 17–18 MΩ cm. Methyltrimethoxysilane (MTMOS, 99%) was purchased from Sigma and used as received. Ultrapure water obtained from a Millipore Milli-Qwater purification system was used throughout the experiments. Solutions with different pH (0.10–4.86) were prepared by mixing the 0.1 M Na_2SO_4 aqueous solution with the 0.1 M Na_2SO_4 + 0.5 M H_2SO_4 aqueous solution. Solutions were deaerated by argon bubbling prior to the experiments and the electrochemical cell was kept under argon atmosphere throughout the experiments.

2.2. Characterization of the films

Atomic force microscopy (AFM) images were taken on mica slides using a Nanoscope IIIa instrument (Digital Instruments) operating in the tapping mode with silicon nitride tips. UV–VIS absorption spectra were recorded on a quartz slide using a 756CRT UV–VIS spectrophotometer. X-ray photoelectron spectra (XPS) were measured on a silicon wafer using an Escalab-MK II photoelectronic spectrometer with ALK2 (1486.6 eV) as excitation source. A CHI 600 electrochemical workstation connected to a digital-586 personal computer was used for control of the electrochemical measurements and for data collection. A conventional three-electrode system was used. The working electrode was a $(Mo_{38})_n$/PAH composite film modified WIGE electrode and a WIGE. A SCE was used as the reference electrode and Pt gauze as a counter electrode. The WIGE was polished with 1, 0.5 and 0.1 μm α-Al_2O_3 paste, respectively, washed with distilled water then ultrasonicated in deionized water and acetone successively. A pHS-25B type pH meter was used for pH measurement.

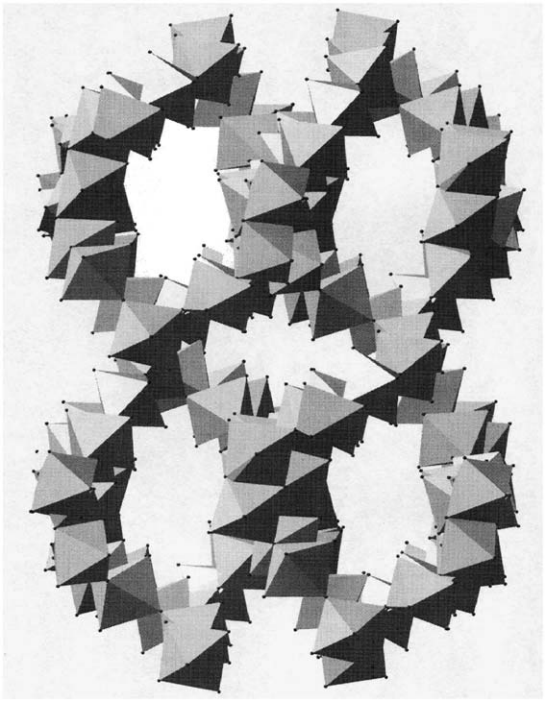

Fig. 1. Chemical structure of the wheel-shaped molybdenum polyoxometalate cluster $(Mo_{38})_n$ used in this work.

2.3. Preparation of self-assembly films

The fabrication of $(Mo_{38})_n$ is illustrated in Fig. 1 and is described as follows. The substrates (quartz or silicon) were all cleaned by first placing them in a hot H_2SO_4/H_2O_2 (7:3) bath for 40 min and then in an H_2O/H_2O_2/NH_4OH (5:1:1) bath for 30 min. The cleaned substrates were immersed in a 10^{-2} M PEI solution (pH = 9) for 20 min, rinsed with water, and dried under a nitrogen stream. In the aqueous solution of pH = 9, at least 3% of the amino group in PEI is protonated, resulting in that PEI acts as polycation. The PEI-coated substrates were then exposed to a 10^{-2} M PSS solution for 20 min, followed by alternating 20 min immersions in 10^{-2} M PAH solution (containing 1 M NaCl; pH = ~1.5–4.5) and $(Mo_{38})_4$ (1×10^{-3} M, pH = ~3.5–4.5) solutions. Water rinses and nitrogen drying steps were performed after each adsorption step (see Fig. 2).

3. Results and discussion

UV–VIS spectroscopy is used to monitor the deposition process. Fig. 3 shows the UV–VIS spectra of $((Mo_{38})_n$/PAH$)m$ multilayers ($m = 0-6$) deposited on a precursor (PEI/PSS/PAH) film on a quartz substrate. In the films preparation, the presence of these two sublayers of PEI/PSS can firm the interfacial linkage between the substrate and the films. The absorption band at 225 nm in the UV–VIS spectrum of the precursor (PEI/PSS/PAH) film arises from the aromatic group present in the PSS polyanion. Because the UV–VIS spectrum of an aqueous $(Mo_{38})_n$ solution indicates three absorption bands at 209, 267 and 300 nm, so we utilized these absorption bands to monitor film growth. For the UV-VIS spectrum of the multiplayer films, the

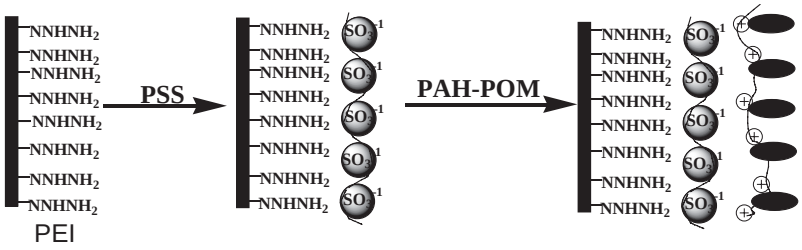

Fig. 2. Schematic diagram of the formation of the multilayer structure of polyelectrolytes (PEI/PSS/PAH) and $(Mo_{38})_n$ anion clusters on substrates.

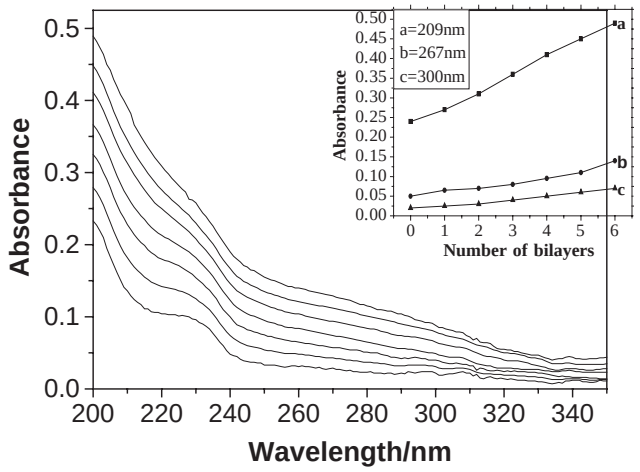

Fig. 3. UV-VIS spectra of the $((Mo_{38})_n/PAH)_m$ composite films with $m = 0$ and 6.

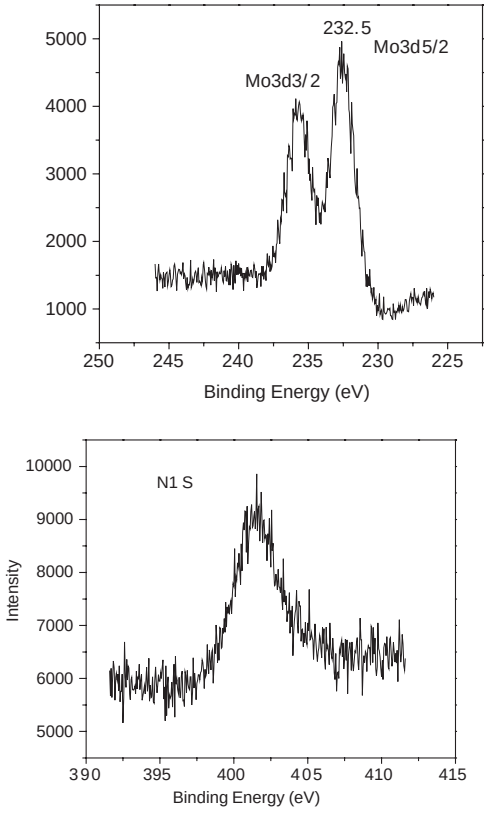

Fig. 4. X-ray photoelectron spectra in the N(1 s) and Mo(3*d*) regions for the $((Mo_{38})_n/PAH)_m$ composite films with $m = 4$.

absorbance maxima at 267 or 300 nm cannot be observed clearly. However, plotting the $((Mo_{38})_n/PAH)_m$ layers still results in nearly straight lines, which confirms constant incorporation of $(Mo_{38})_n$ in the multiplayer. The gradual increase of absorbance in UV–VIS spectra (see Fig. 3) shows a clear evidence that a full layer absorption has arisen after each step. The polycation PAH does not absorb above 200 nm, and its presence in the film does not contribute to the absorption spectra. A partial loss of $(Mo_{38})_n$ clusters after each PAH deposition step is observed in the UV–VIS spectra, but the steady increase in the absorbance demonstrates that $(Mo_{38})_n$ anions are deposited in the multilayer films.

To identify the elemental composition of the multilayer films, we measured the XPS of the $((Mo_{38})_n/PAH)m$ ($m = 4$) films. Although the XPS measurement gives only semi-quantitative elemental composition, the presence of C, O, N, S, P, and Mo elements in the film is confirmed. The XPS of the $((Mo_{38})_n/PAH)m$ films ($m = 4$) are shown in Fig. 4.We observe that the peak intensities of the Mo3*d* and N1s levels (at 232.5 and 401.2 ev, respectively) increase with the increasing number of $((Mo_{38})_n/PAH)_m$ bilayers. The observed variation of the relevant peak intensities with successive deposition is clearly indicative of the constant film growth as a result of LbL deposition, in agreement with the UV–VIS spectra. Furthermore, the presence of a single N1s peak in the XPS measurement reflects that the valence state of the nitrogen atoms from PAH does not change after LbL deposition; this indicates that only a simple electrostatic interaction exists between the layers.

The AFM images of the PEI/PSS/PAH precursor film and an additional bilayer of $(Mo_{38})_n/PAH$, were taken to provide detailed information about the surface morphology and the homogeneity of the deposited films (see Fig. 5). Before $(Mo_{38})_n$ adsorption, the outer PAH surface layer of the precursor film is uniform and smooth, with a mean roughness of 0.414 nm. After adsorption of $(Mo_{38})_n$, followed by adsorption of a PAH

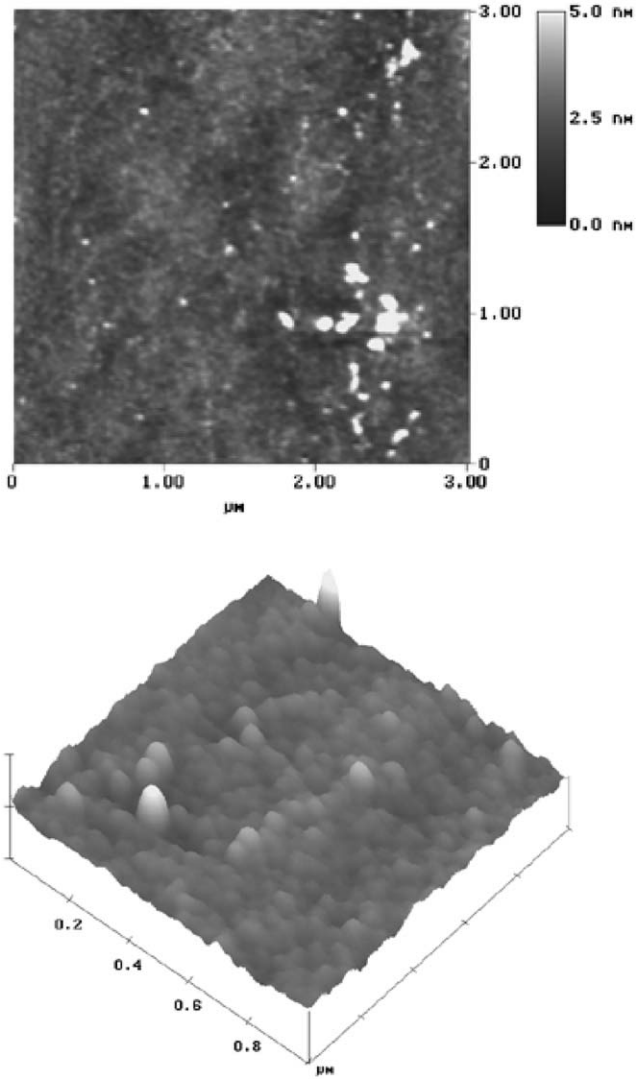

Fig. 5. Tapping mode AFM images of [(PEI/PSS/PAH)$((Mo_{38})_n$/PAH$)_m$] films.

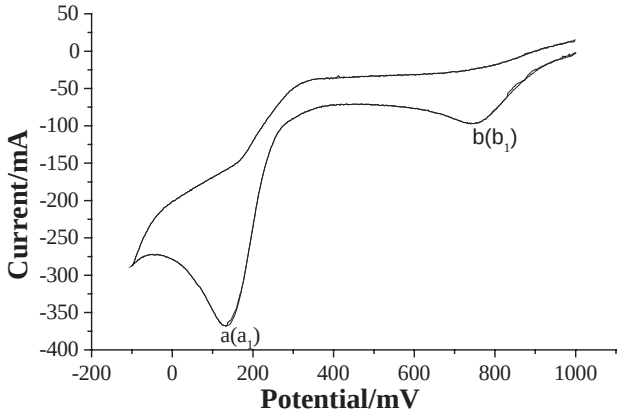

Fig. 6. Cyclic voltammograms of the $((Mo_{38})_n/PAH)_m$ composite film modified WIGE electrode and bared-electrode Scan rate: $20\,mV\,s^{-1}$ $(m = 4)$.

surface layer, the mean interface roughness has increased to 1.947 nm. In addition, the AFM image of this sample shows an almost uniform distribution of aggregated nanoclusters (see Fig. 5). This should be explained not only as a result of PAH deposition but also as an indirect reflection of $(Mo_{38})_n$ cluster. X-ray reflectance date was collected for the multilayer films in order to investigate their structure, but no Kiessig fringes appear in the XRR curve, indicating that the film surface is inhomegeneous. In fact, a strict lamellar structure with sharp interfacial confinements between $(Mo_{38})_n$ and PAH layers is almost impossible to reach [20]. Therefore, AFM images were used to estimate the thickness of the film. The estimated thickness of [(PEI/PSS/PAH)$((Mo_{38})_n$/PAH$)_m$] multilayer films is ca. 3.7 nm.

To our knowledge there is no report on the preparation and electrochemical behavior study of (the wheel-shaped molybdenum polyoxometalate cluster $((Mo_{38})_n/PAH)_m$ composite film modified WIGE electrode (wax impregnated graphite electrode). We first prepared a new kind of the $((Mo_{38})_n/PAH)_m$ composite films modified WIGE electrode. The $((Mo_{38})_n/PAH)_m$ composite films modified WIGE electrode has good stability. The stability of the composite film electrode was examined by measuring the increase in voltammetric currents of the composite film electrode during potential cycling. For example, the film electrode was subjected in 1 M H_2SO_4 solution to 100 potential cycles in the potential range of 0.6 and -0.1 V at $100\,mV\,s^{-1}$, a decrease in the cathodic current of less than 10% was observed. After soaking the $((Mo_{38})_n/PAH)_m$ composite films modified WIGE electrode in 1 M H_2SO_4 solution for 10 days, almost no change of the electrochemical response of $(Mo_{38})_n$ was observed. This shows that a significant activation barrier impedes the break-up of the electrostatic binding within the composite film. Fig. 6 shows cyclic voltammograms of the composite film electrode prepared from 2 M $H_2SO_4 + 5$ mM $(Mo_{38})_n$ liquor and bared-electrode in 2 M $H_2SO_4 + 5$ mM $(Mo_{38})_n$ liquor at $20\,mV\,s^{-1}$scan rate, and the peaks show two irreversible reduction steps at 148 and at 758 mV. The peaks reveal that the electrochemical behavior of the composite film electrode $(Mo_{38})_n$ is similar as bared-electrode in 2 M $H_2SO_4 + 5$ mM $(Mo_{38})_n$ liquor. Experiments are in progress to investigate electrochemica behavior of the $((Mo_{38})_n/PAH)_m$ composite films modified WIGE electrode.

4. Conclusions

In the present work, it has been shown that highly ordered $((Mo_{38})_n/PAH)_m$ multilayers films can be successfully fabricated on solid substrates using consecutive

LbL electrostatic adsorption. The ultrathin multilayer film has been characterized by UV–VIS spectroscopy, small-angle X-ray reflectivity measurements, XPS, and AFM image method. These researches reveal both the regular film growth with each $(Mo_{38})_n$ adsorption and the film thickness at nanoscale (ca. 3.7 nm). The occurrence of the electrochemical properties confirms the potential for creating multilayer films with POMs. Work is in progress on investigate of applicability of $((Mo_{38})_n/PAH)_m$ multilayer films for device applications.

Acknowledgments

This project was financially supported by the National Natural Science Foundation of China (Grant no. 20171010).

References

[1] H. Krass, G. Papastavrou, D.G. Kurth, Chem. Mater. 15 (2003) 196.
[2] A. Ulman, Introduction to Thin Films: From Langmuir–Blodgett to Self-assembly, Academic Press, Boston, 1991.
[3] G. Decher, Science 277 (1997) 1232.
[4] J. Schmitt, G. Decher, W.J. Dressick, S.L. Brandow, R.E. Geer, R. Shashidhar, J.M. Calvert, Adv. Mater. 9 (1997) 61.
[5] A.K. Dutta, T. Ho, L. Zhang, P. Stroeve, Chem. Mater. 12 (2000) 1042.
[6] S.L. Clark, E.S. Handy, M.F. Rubner, P.H. Hammond, Adv. Mater. 11 (1999) 103.
[7] X. Zhang, J.C. Shen, Adv. Mater. 11 (1999) 1139.
[8] J.A. He, R. Valluzzu, K. Yang, T. Dolukhanyan, C.M. Sung, J. Kumar, S.K. Tripathy, L.A. Samuelson, L. Balogh, D.A. Tomalia, Chem. Mater. 11 (1999) 3268.
[9] I. Pastoriza-Santos, D.S. Koktysh, A.A. Mamedov, M. Giersig, N.A. Kotov, L.M. Liz-Marzan, Langmuir 16 (2000) 2731.
[10] (a) L. Wang, Z. Liu, Y. Zhou, E.B. Wang, J. Chin. Univ. 18 (6) (1997) 846;
(b) Xiuli Wang, Enbo Wang Yanglan, Changwen Hu, Electroanalysis 14 (2002) 1116;
(c) Xiuli Wang, Zhenhui Kang, Enbo Wang, Changwen Hu, J. Electroanal. Chem. V523 (1–2) (2002) 142;
(d) Xiuli Wang, Enbo Wang, Changwen Hu, Chem. Lett. (2001) 1030.
(e) H.Y. Zhang, L. Xu, E.B. Wang, M. Jiang, A.G. Wu, Z. Li, Mater. Lett. 57 (2003) 1417.
[11] C. Hu, Y. Zhang, L. Xu, Appl. Catal. A 177 (1999) 237.
[12] G. Liu, Y. Wei, Q. Yu, Q. Liu, S. Zhang, Inorg. Chem. Commun. 2 (1999) 434.
[13] A. Müller, E. Krickemeyer, H. Bögge, M. Schmidtmann, F. Peters, C. Menke, J. Meyer, Angew. Chem. 109 (1997) 500.
[14] A. Müller, E. Krickemeyer, H. Bögge, M. Schmidtmann, F. Peters, C. Menke, J. Meyer, Angew. Chem. Int. Ed. Engl. 36 (1997) 484.
[15] D.G. Kurth, P. Lehmann, D. Volkmer, A. Müller, D. Schwahn, J. Chem. Soc., Dalton Trans. 21 (2000) 3989.
[16] I. Ichinose, H. Tagawa, H. Mizuki, Y. Lvov, T. Kunitake, Langmuir 14 (1998) 3462.
[17] F. Caruso, D.G. Kurth, D. Volkmer, M.J. Koop, A. Müller, Langmuir 14 (1998) 187.
[18] D.G. Kurth, D. Volkmer, M. Ruttorf, B. Richter, A. Müller, Chem. Mater. 12 (2000) 2829.
[19] S. Zhang, D. Qing, M. Shao, Y. Tang, J. Chem. Soc., Chem. Commun. (1986) 835.
[20] L. Xu, H. Zhang, E.B. Wang, D.G. Kurth, Z. Li, J. Mater. Chem. 12 (2002) 654.
[21] S. Liu, D.G. Kurth, B. Bredenkotter, D. Volkmer, J. Am. Chem. Soc. 124 (41) (2002) 12279.